Soft Matter

PAPER

View Article Online
View Journal | View Issue

Cite this: *Soft Matter*, 2017, 13, 2448

Optothermally driven colloidal transport in a confined nematic liquid crystal†

M. Škarabot,*[a] N. Osterman[ab] and I. Muševič[ab]

Received 19th January 2017,
Accepted 2nd March 2017

DOI: 10.1039/c7sm00136c

rsc.li/soft-matter-journal

We demonstrate transport of microparticles by rapid movement of a laser spot in a thin layer of a nematic liquid crystal. The transport is achieved by fluid flow, caused by two different mechanisms. The thermoviscous expansion effect induces colloidal transport in the direction opposite to the laser movement, whereas thermally induced local melting of the liquid crystal pulls the particles in the direction of the laser movement. We demonstrate control of colloidal transport by changing the speed of the laser trap movement and the laser power. We anticipate that complex optofluidic colloidal transport could be realized in the nematic liquid crystal using a channel-free optofluidic approach.

Introduction

Nematic liquid crystals (NLCs) are unique materials with extraordinary optical properties that are widely used in LC display technology. Dispersions of different particles in NLCs have been extensively studied in the last two decades, because they can change and improve the LC properties. A prominent example is ferromagnetism in the dispersion of ferromagnetic nano-platelets in NLCs.[1] NLCs can also be used as anisotropic solvents, which provide structural forces between inclusions that can self-assemble into different 2D and 3D colloidal crystals.[2,3] In order to assemble various colloidal structures in nematic liquid crystals, tools for manipulation and transport of particles are needed. Different methods have been used for colloidal manipulation and transport in NLCs,[4] using an external electric field,[5–8] microfluidics,[9,10] nematic–isotropic interfaces,[11] laser tweezers[12–15] or thermal expansion.[16,17] Of particular interest is laser tweezers manipulation, which provides a precise and well controlled means of manipulating colloidal particles in NLCs. It has been shown that various physical mechanisms are involved in laser tweezing of particles in the NLCs, and among them thermal reduction of the order parameter by the hot spot of the laser tweezers is the strongest and therefore most efficient.[15]

On the other hand, it has been shown in isotropic fluids that the movement of a warm spot, which is generated by the motion of a focused laser beam of the tweezers, induces a fluid flow by thermal expansion and contraction of a viscous fluid. This method can also be used for an efficient transport and trapping of particles in isotropic fluids.[18,19] However, we should stress that the mechanism of particle transport in isotropic fluids by the warm spot of the laser tweezers is quite different compared to the similar effect in the NLCs. In the isotropic fluids, the flow of colloidal particles is due to the flow of the fluid, induced by a thermoviscous expansion effect. This flow is always opposite to the moving direction of the warm spot. On the other hand, colloidal particles can also be moved in NLCs due to the structural force, induced by the spatial gradient of the order parameter.[15] This motion is always along the direction of the warm spot.

In this work we combine both mechanisms by applying a large power of the moving spot of the laser tweezers, which induces local thermal expansion and contraction of the NLCs as well as local reduction of the order parameter. There are therefore two opposing mechanisms of colloidal transport taking place. As a result, we observe colloidal transport, the direction of which depends on the parameters of the moving warm spot. We present the analysis and possible scenarios of colloidal transport for different experimental parameters.

Experimental setup

In the experiments we used homeotropically oriented LC cells made of one optically transparent indium tin oxide (ITO) coated glass and one normal glass. The ITO coating on one substrate was used as an absorber of laser light and it provides very good control of the local LC heating. The thickness of the cells was controlled with Mylar spacers and was set to 4–6 μm. Homeotropic orientation of LC molecules was achieved by covering glass and ITO surfaces with DMOAP silane (ABCR GmbH), which ensures a very strong perpendicular orientation of the LC molecules at the surface. LC cells were filled with nematic liquid crystal E12 (Merck) using a capillary effect. A very

[a] J. Stefan Institute, Jamova 39, SI-1000, Ljubljana, Slovenia. E-mail: miha.skarabot@ijs.si
[b] Faculty of Mathematics and Physics, University of Ljubljana, Jadranska 19, SI-1000, Ljubljana, Slovenia

† Electronic supplementary information (ESI) available. See DOI: 10.1039/c7sm00136c

small amount of silica microspheres with a diameter of 0.97 μm or 2.32 μm (Bangs Laboratories) was dispersed in the LC in order to follow its hydrodynamic flow. Microspheres were treated with the same DMOAP silane which induces strong homeotropic anchoring at the surface of the particles.

Hydrodynamic flow of the LC was induced by moving a focused IR laser beam, which was achieved by a pair of acousto-optic deflectors controlled by a computerized laser tweezers system (Aresis, Tweez 70) built around an inverted optical microscope (Nikon Eclipse, TE2000-U) and an IR fiber laser. The microparticles were video recorded using the PixeLINK PL-A741 camera at a frame rate of 40 frames per second. In an off-line analysis, the time dependence of microparticle positions was determined by using a video-tracking procedure with a typical resolution of particle positions ±15 nm and consequently the velocity of the microparticles was determined by numerical derivation of the trajectory as a function of time. The orientation of the LC molecules was observed between crossed polarizers with a full wave plate inserted between the analyzer and the sample, while color images were taken with a Canon EOS 500 camera.

Results and discussion

In the experiment the laser spot was moving along a circular trajectory with a radius of 10 μm (Fig. 1a). The NLC is heated due to the absorption of the laser light at the ITO surface, but since the applied laser power is rather small ($P \sim 45$ mW), the NLC is not heated to the isotropic phase. We observe in the experiment that small colloidal particles circulate in the opposite direction with respect to the circulation of the laser trap, as illustrated in Fig. 1a. This effect is well known for isotropic fluids, such as water,[18] and is due to the thermoviscous expansion and consequent contraction of the fluid under the local heat dissipation of the moving warm spot of the laser tweezers. The velocity of the particle is always opposite to the trap movement and is equal to the flow velocity v, which is determined by the following expression:[18]

$$v = -\frac{3\sqrt{\pi}}{4} f \alpha \beta b \Delta T^2. \quad (1)$$

Here f is the circulation frequency of the laser spot, α is the coefficient of thermal expansion, β describes the temperature dependence of viscosity ($\beta = (1/\eta)(\partial\eta/\partial T)$), b is the width of the warm spot and ΔT is the increase of the temperature in the centre of the spot. We checked the validity of eqn (1) in the E12 nematic LC and the flow velocity is indeed proportional to the laser rotation frequency (Fig. 1b), as predicted. It should be noted that the velocity of the induced flow is several orders of magnitude lower than the velocity of the laser spot. The flow has the direction opposite to the laser spot movement, as described by a minus sign in eqn (1). To estimate ΔT, we used $\alpha = 15 \times 10^{-4}$ K^{-1},[20] $\beta = 0.065 \times 10^{-4}$ K^{-1},[21] $b = 10$ μm, and we obtained $\Delta T \approx 3$ K. We checked the estimated increase of temperature ΔT in a separate experiment by observing the fluorescence of the dispersed dye, which has the emission spectra dependent on temperature.[22] We used the 5CB doped with the dispersed dye in the same cell during illumination of the sample and we obtained slightly larger $\Delta T \approx 4$ K. It is interesting that no LC reorientation due to the nematic flow can be observed in this case (Fig. 1c). This is a consequence of thin LC cells with strong homeotropic anchoring and relatively slow flow velocity of the order of 1 μm s^{-1}. It has been shown in the microfluidic experiment that in this geometry the LC reorientation occurs at a velocity of above 10 μm s^{-1}.[23]

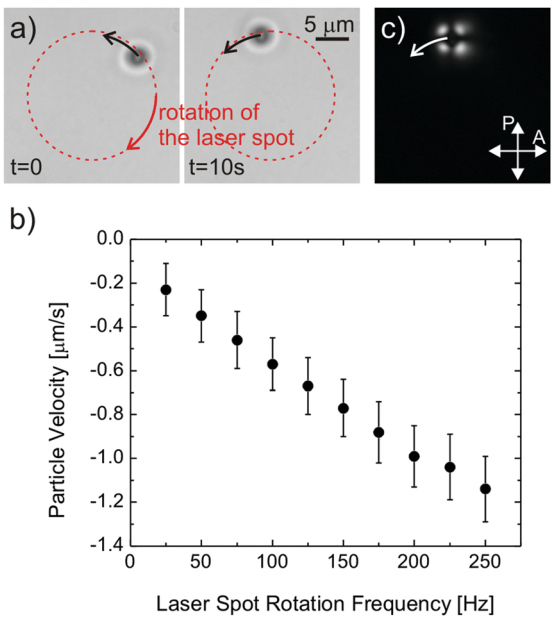

Fig. 1 Circulation of the laser spot induces hydrodynamic flow in the E12 nematic LC. (a) When a small laser power is used ($P \approx 45$ mW), the 2.3 μm colloidal particle circulates along the direction of the nematic flow (black arrow), which is opposite to the circulation of the laser spot (red arrow). (b) The particle velocity is proportional to the laser circulation frequency. (c) No LC reorientation can be observed between crossed polarizers due to the liquid crystal flow at a low laser power.

In the next experiment we increased the laser power and the liquid crystal was locally heated to the isotropic phase, thus forming a small isotropic island. This molten and isotropic island can be observed under an optical microscope as a small bright spot around the position of the laser spot in Fig. 2a. It is well known that such an isotropic droplet strongly attracts colloidal particles for two reasons: (i) by elastic forces due to the decreased order parameter in the heated region and (ii) by the nematic–isotropic (NI) interface.[14,15] Both mechanisms always attract particles towards the isotropic island and therefore move together with a moving laser spot. We observed by analysing captured video frames that the particle does not move continuously with the laser spot, but it is pulled by the moving laser tweezers for a certain distance in each cycle of circulation.

The nematic flow induced by the thermoviscous effect in the direction opposite to the laser spot movement is still present, but at a low frequency of the laser spot rotation the pulling effect on average overcomes the flow effect and the particle moves in the direction of the laser spot (Fig. 2a). Actually the particle undergoes oscillatory motion since it is pulled by an

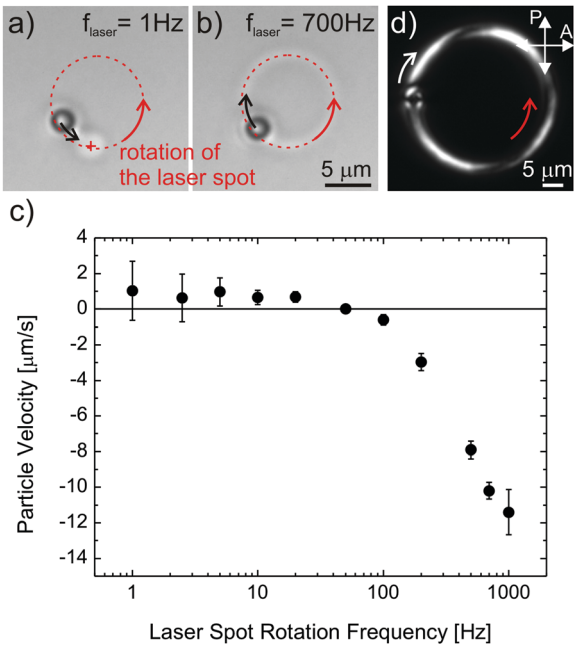

Fig. 2 The laser spot at a stronger power ($P \approx 60$ mW) locally heats the LC to the isotropic phase. (a) At a small laser circulation frequency ($f < 30$ Hz) the 2.3 μm colloidal particle is pulled by the isotropic droplet in the direction of the laser movement. (b) At a higher rotation frequency ($f > 60$ Hz) the particle moves in the opposite direction due to the thermoviscous effect. (c) The velocity of a particle as a function of the laser circulation frequency. (d) The movement of the isotropic droplet induces LC reorientation, visible between crossed polarizers.

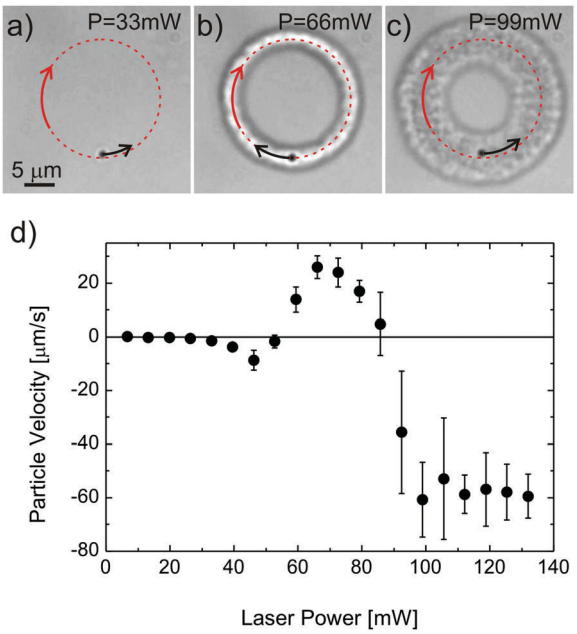

Fig. 3 Movement of the 1 μm particle in the LC induced by the circulation of the laser spot at a fixed frequency (f = 1 kHz) depends on the power at the laser spot. (a) At low power the particle moves opposite to the laser movement, (b) at intermediate power along the laser movement and (c) at high power again opposite to the laser movement. (d) The particle velocity strongly depends on the laser power.

isotropic island for a small distance in the direction of the laser movement, but then it is moved back in the direction of the nematic flow. These oscillations are observed only at small laser spot frequencies ($f < 10$ Hz) and in the graphs only the average velocity of the particle is presented. When the rotation frequency is increased, the thermoviscous flow effect is increased and the particle moves in the direction opposite to the laser movement (Fig. 2b). As a result of two competing mechanisms of colloidal transport, we can control the direction and the speed of the particle movement simply by changing the laser circulation frequency (Fig. 2c). The movement of the small isotropic droplet with a high speed induces transient NLC reorientation, which can be observed under a polarizing microscope (Fig. 2d) and it will be discussed in detail later in this work.

In the next set of experiments we kept the laser circulation frequency fixed (f = 1 kHz) and the laser power was increased in discrete steps. Here we observed three different regimes of the particle movement depending on the laser power P:

- $P < 50$ mW: only the thermoviscous effect is present and the particle moves opposite to the direction of the laser spot (Fig. 3a).
- 50 mW $< P <$ 90 mW: the LC is locally heated to the isotropic phase and the isotropic droplet pulls the particle in its direction (Fig. 3b).
- $P >$ 90 mW: the LC is heated in the isotropic phase continuously in the whole region of the laser spot rotation. There is no isotropic droplet and therefore no pulling effect. The thermoviscous effect is only present and the particle moves opposite to the direction of the laser spot like in a normal isotropic fluid (Fig. 3c).

By changing the laser power at a fixed laser circulation frequency, the colloidal movement can be fully controlled (Fig. 3d). While the nematic flow is always opposite to the direction of the laser spot, the particle can move in the direction of the nematic flow or exactly opposite to it due to the pulling effect of the thermally induced isotropic droplet. It should be noted that all the observed effects strongly depend on the heating of the NLC. Here we used homeotropic LC cells with one ITO coated substrate, which strongly absorbs laser light and consequently the LC is heated. If both substrates were normal microscopic glass substrates without ITO, the heating would be less effective and the same effects were observed at almost one magnitude higher laser power. When sapphire glass substrates were used, which absorb much less IR light than glass substrates, no heating of the LC was observed also at a very high laser power (P = 800 mW), and consequently there was no induced nematic flow. The strength of the pulling effect by the isotropic droplet depends on the size of the LC distortion induced by the particle and on the gradient of the order parameter around the hot spot. In our case this distortion is relatively big since we use particles with strong surface anchoring. The maximal velocity of 1 μm particles caused by the pulling effect is around 25 μm s^{-1}, which means that the maximal trapping force of the isotropic droplet is approx. 10 pN. In the case of particles with weak anchoring the trapping of particles by the isotropic droplet is weaker and the pulling effect is less pronounced.

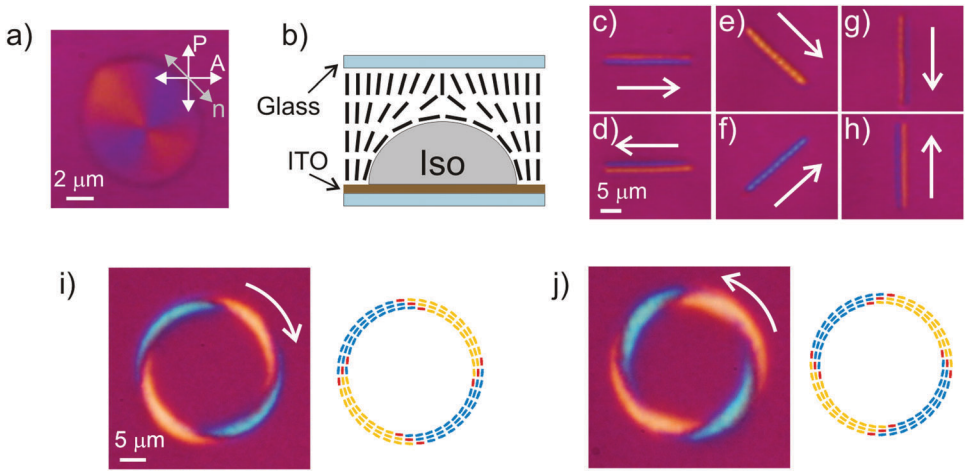

Fig. 4 (a) Reorientation of LC molecules induced by the molten and isotropic droplet of E12, observed with the polarizing microscope with a λ-plate. *P* and *A* show the orientations of the polarizer and the analyser and *n* is the direction of the optical axis of the λ-plate. The laser spot does not move and is switched on and off with a frequency of 5 kHz and a power of 170 mW. As a result, an isotropic droplet is induced on the ITO coated glass substrate and the LC molecules are oriented planarly at the NI interface (b). (c–h) The laser spot is continuously moved in different directions (f = 1 kHz, P = 55 mW). In this way an isotropic line on the ITO coated substrate is formed and the orientation of the molecules and the corresponding colours are dictated by the tail part of the droplet. (i and j) Laser spot rotates in a circle (f = 1 kHz, P = 60 mW) and an isotropic torus is created on the ITO coated substrate. As a result, tilted molecules are observed at the interface of the isotropic torus and the nematic E12, which are also schematically presented for both senses of circulation.

Finally, we were interested in the reorientation of the LC director, which is induced by the laser spot movement and by the LC flow. It is interesting that at a low laser power no reorientation can be observed; nevertheless, the flow of the nematic LC is present (Fig. 1c). When the laser power is increased, the LC is locally heated to the isotropic phase and LC reorientation becomes visible (Fig. 2d), which can be studied in detail using a polarizing microscope with an additional full wave plate λ = 530 nm (Fig. 4). By using this plate we can distinguish between two orientations of the LC molecules, deflected for the same angle in two different directions. With this plate these two directions appear bluish or yellowish, while without this plate they both appear white, as one can see by comparing Fig. 2d and 4j, which present the same experiment. Because in the experiment the laser spot is switched between neighboring positions at a high frequency, we first checked the effect of fast on–off switching of the laser at a fixed position. This is shown in Fig. 4a, where the laser spot is stationary and is switched on and off with a frequency of 5 kHz. The isotropic droplet is formed from the hot ITO surface, but does not extend throughout the whole thickness of the cell. If this was the case, then the circle in Fig. 4a would be of uniform red colour without yellow and blue sections. Because there is a planar orientation of E12 on its isotropic border, the cross-section of the isotropic E12 droplet surrounded by the nematic E12 is illustrated in the schematics in Fig. 4b. Actually looking at the isotropic droplet from the top, we see reorientation from the bulk homeotropic orientation to the planar tilted orientation at the NI interface.

When such a droplet is moved with a high speed through the LC, it leaves behind a temporarily reoriented nematic, giving characteristic yellow and blue sections under a polarizing microscope with the λ-plate. Fig. 4c shows an example of the laser spot scanned from the left to the right with a repetition frequency of 1 kHz. The LC molecules are reoriented in the direction dictated by the tail part of the droplet[24] and one can see the yellow color at the top and the blue color at the bottom part of the line. When the direction of the line is reversed, the tilt of the molecules and the colours are also reversed (Fig. 4d). In the next case the laser spot is moved under 45 degrees in the SE (south-east) direction, LC molecules are reoriented in the same direction and consequently the yellow color appears according to Fig. 4a (Fig. 4e). When the direction is changed to NE, the color is changed to blue (Fig. 4f). In the last case the spot moves in the vertical direction and the colours of the lines can be easily predicted according to the direction of the movement (Fig. 4g and h). Finally, the laser spot continuously circulated in the clockwise and counter-clockwise directions (Fig. 4i and j). The reorientation of the LC molecules (and consequently the observed colours) always follows the orientation at the tail part of the thermally induced isotropic droplet. It should be emphasized here that thermally induced nematic flow does not induce reorientation of LC molecules as can be seen in Fig. 1c and 3a. The reorientation is induced only by the isotropic droplet when a higher laser power is used.

Conclusion

This work demonstrates two different mechanisms of colloidal transport induced by the fast movement of the warm spot of the laser tweezers. The transport of particles is achieved by two thermal effects, which induce colloidal transport in two opposite directions. The thermoviscous expansion effect induces fluid

flow and colloidal transport in the opposite direction of laser movement, while pulling by a thermally induced isotropic droplet of a nematic induces colloidal transport in the direction of laser movement. In the present work the local heating of the LC is achieved by the absorption of the laser light at the substrate surfaces in thin nematic cells, so the flow and the transport are restricted to 2D. To expand the method to 3D with a complex flow configuration, other methods should be used as well, like LC dispersions of nanoparticles, which can absorb the light and locally heat the LC. We also anticipate that complex microfluidic circuits with channel-free colloidal transport could be achieved in nematic LCs by contactless optical control.

Acknowledgements

The authors acknowledge financial support from the Slovenian Research Agency (ARRS) through contracts P1-0099, J1-6723 and J1-6724.

References

1 A. Mertelj, D. Lisjak, M. Drofenik and M. Čopič, *Nature*, 2013, **504**, 237–241.
2 I. Muševič, M. Škarabot, U. Tkalec, M. Ravnik and S. Žumer, *Science*, 2006, **313**, 954–958.
3 A. Nych, U. Ognysta, M. Škarabot, M. Ravnik, S. Žumer and I. Muševič, *Nat. Commun.*, 2013, **4**, 1489.
4 O. D. Lavrentovich, *Soft Matter*, 2010, **10**, 1264–1283.
5 M. Škarabot, U. Tkalec and I. Muševič, *Eur. Phys. J. E: Soft Matter Biol. Phys.*, 2006, **24**, 99–107.
6 O. P. Pishnyak, S. Tang, J. R. Kelly, S. V. Shiyanovskii and O. D. Lavrentovich, *Phys. Rev. Lett.*, 2007, **99**, 127802.
7 O. D. Lavrentovich, I. Lazo and O. P. Pishnyak, *Nature*, 2010, **467**, 947–950.
8 A. V. Ryzhkova, F. V. Podgornov and W. Haase, *Appl. Phys. Lett.*, 2010, **96**, 151901.
9 A. Sengupta, U. Tkalec and C. Bahr, *Soft Matter*, 2011, **7**, 6542–6549.
10 A. Sengupta, S. Herminghaus and C. Bahr, *Liq. Cryst. Rev.*, 2014, **2**, 73–110.
11 J. L. West, A. Glushchenko, G. Liao, Y. Reznikov, D. Andrienko and M. P. Allen, *Phys. Rev. E: Stat., Nonlinear, Soft Matter Phys.*, 2002, **66**, 012702.
12 I. Muševič, M. Škarabot, D. Babič, N. Osterman, I. Poberaj, V. Nazarenko and A. Nych, *Phys. Rev. Lett.*, 2004, **93**, 187801.
13 I. I. Smalyukh, A. N. Kuzmin, A. V. Kachynski, P. N. Prasad and O. D. Lavrentovich, *Appl. Phys. Lett.*, 2005, **86**, 021913.
14 S. A. Tatarkova, D. R. Burnham, A. K. Kirby, G. D. Love and E. M. Terentjev, *Phys. Rev. Lett.*, 2007, **98**, 157801.
15 M. Škarabot, Ž. Lokar and I. Muševič, *Phys. Rev. E: Stat., Nonlinear, Soft Matter Phys.*, 2013, **87**, 062501.
16 Y. K. Kim, B. Senyuk and O. D. Lavrentovich, *Nat. Commun.*, 2012, **3**, 1133.
17 Y. Takenaka and T. Yamamoto, *Soft Matter*, 2017, **13**, 1116.
18 F. M. Weinert, J. A. Kraus, T. Franosch and D. Braun, *Phys. Rev. Lett.*, 2008, **100**, 164501.
19 F. M. Weinert and D. Braun, *J. Appl. Phys.*, 2008, **104**, 104701; N. Osterman and D. Braun, *Appl. Phys. Lett.*, 2015, **106**, 073508.
20 S. Weiss and G. Ahlers, *J. Fluid Mech.*, 2013, **737**, 308–328.
21 M. Cui and J. R. Kelly, *Mol. Cryst. Liq. Cryst.*, 1999, **331**, 1909–1917.
22 C. B. Mast and D. Braun, *Phys. Rev. Lett.*, 2010, **104**, 188102.
23 A. Sengupta, U. Tkalec, M. Ravnik, J. M. Yeomans, C. Bahr and S. Heminghaus, *Phys. Rev. Lett.*, 2013, **110**, 048303.
24 G. Mirri, M. Škarabot and I. Muševič, *Soft Matter*, 2015, **11**, 3347.

